Journal of Power Sources 192 (2009) 360–366

Contents lists available at ScienceDirect

Journal of Power Sources

journal homepage: www.elsevier.com/locate/jpowsour

Self-sustained operation of a kW_e-class kerosene-reforming processor for solid oxide fuel cells

Sangho Yoon [a], Joongmyeon Bae [a,*], Sunyoung Kim [a], Young-Sung Yoo [b]

[a] Department of Mechanical Engineering, KAIST, 335 Gwahangno, Yuseong-gu, Daejeon 305-701, Republic of Korea
[b] Renewable Energy Research Group, Strategic Technology Laboratory, Korea Electric Power Research Institute, Korea Electric Power Corporation, 103-16 Munji-Dong, Yuseong-Gu, Daejon 305-380, Republic of Korea

ARTICLE INFO

Article history:
Received 19 November 2008
Received in revised form 3 February 2009
Accepted 16 February 2009
Available online 13 March 2009

Keywords:
Hydrogen
Kerosene
Autothermal reforming (ATR)
Desulfurizer

ABSTRACT

In this paper, fuel-processing technologies are developed for application in residential power generation (RPG) in solid oxide fuel cells (SOFCs). Kerosene is selected as the fuel because of its high hydrogen density and because of the established infrastructure that already exists in South Korea. A kerosene fuel processor with two different reaction stages, autothermal reforming (ATR) and adsorptive desulfurization reactions, is developed for SOFC operations. ATR is suited to the reforming of liquid hydrocarbon fuels because oxygen-aided reactions can break the aromatics in the fuel and steam can suppress carbon deposition during the reforming reaction. ATR can also be implemented as a self-sustaining reactor due to the exothermicity of the reaction. The kW_e self-sustained kerosene fuel processor, including the desulfurizer, operates for about 250 h in this study. This fuel processor does not require a heat exchanger between the ATR reactor and the desulfurizer or electric equipment for heat supply and fuel or water vaporization because a suitable temperature of the ATR reformate is reached for H_2S adsorption on the ZnO catalyst beds in desulfurizer. Although the CH_4 concentration in the reformate gas of the fuel processor is higher due to the lower temperature of ATR tail gas, SOFCs can directly use CH_4 as a fuel with the addition of sufficient steam feeds ($H_2O/CH_4 \geq 1.5$), in contrast to low-temperature fuel cells. The reforming efficiency of the fuel processor is about 60%, and the desulfurizer removed H_2S to a sufficient level to allow for the operation of SOFCs.

Published by Elsevier B.V.

1. Introduction

Hydrogen is widely considered as a clean energy carrier for the future [1–3]. The reforming processes of hydrocarbon fuels to produce hydrogen via either steam reforming, partial oxidation (POx), or autothermal reforming (ATR, combined SR and POx reaction) are recognized as commercially competitive methods [4,5].

A fuel cell is an electrochemical device that directly converts the chemical energy from the reaction of hydrogen with an oxidant into electrical energy [6]. Fuel cells have become one of the most promising types of power sources for future applications because of their high efficiency and ultra-low emission of environmentally harmful gases. Among the several fuel cell types, solid oxide fuel cells (SOFCs) are operated at high temperature ranges of 600–1000 °C. SOFCs have some advantages in terms of high efficiency, durability, and fuel flexibility. Unlike proton exchange membrane fuel cells (PEMFCs) and low-temperature fuel cells, SOFCs can directly use CH_4 as well as CO as fuels with the addition of sufficient steam feeds. The use of CO and CH_4 is possible because the anode material of SOFCs is capable of steam reforming (SR) [Eq. (1)] and because of the water–gas shift (WGS) [Eq. (2)] reactions [7]:

$$CH_4 + 2H_2O \rightarrow CO_2 + 4H_2 \quad (1)$$

$$CO + H_2O \rightarrow CO_2 + H_2 \quad (2)$$

The hydrogen/syngas produced from liquid hydrocarbon fuel reforming is fit for SOFCs operations. The reformate gas of liquid hydrocarbon fuels (gasoline, kerosene, and diesel) contains higher concentrations of light hydrocarbons, such as methane, ethylene, and ethane, than other hydrocarbon fuels (methane, NG, and LPG). However, the drawbacks are that the operation of liquid hydrocarbon fuel-based SOFCs leads to carbon deposition and sulfur poisoning on the reforming catalyst and the SOFC anode. Therefore, fuel reformers and SOFC anodes need a high tolerance to carbon deposition and sulfur poisoning.

Among several reforming methods, ATR is suitable for liquid hydrocarbon fuel reforming because oxygen-aided reactions can break the aromatics in the fuel and because steam can suppress carbon deposition during reforming reactions [8,9]. Precious metals constitute general catalysts for liquid fuel ATR and are more

* Corresponding author. Tel.: +82 42 350 3045; fax: +82 42 350 8207.
E-mail address: jmbae@kaist.ac.kr (J. Bae).

0378-7753/$ – see front matter. Published by Elsevier B.V.
doi:10.1016/j.jpowsour.2009.02.084

sulfur-tolerant than Ni-based reforming catalysts. We chose an ATR methodology and precious metal catalysts for reforming. However, precious metals are still susceptible to poisoning by even low parts per million (ppm) concentrations of sulfur compounds [10]. Thus, low-sulfur kerosene (about 10 wt. ppm) was selected as the fuel in this study because it contains less sulfur compounds than other commercial liquid fuels in South Korea.

Nevertheless, a desulfurizer is still required for stable SOFC operations. Indeed, the H_2S present in the kerosene reformate gas is considered as the primary sulfur poison for Ni in SOFC anode material. During reforming operations, the sulfur, which is initially present as organosulfur compounds, is primarily converted into H_2S. The desulfurizer is one of the key factors in a fuel processor since it allows elimination of the hydrogen sulfide in the reformate gas.

We first investigate the performance of the desulfurizer with liquid fuel reforming in a microreactor system. The individual operation of a kW_e-class kerosene ATR is then tested to determine the temperature of the reformate gas. If the temperature of the reformate gas is adequate for the adsorptive desulfurization reaction, it is possible to drive a self-sustaining kerosene processor without using a heat exchanger to operate the desulfurizer. Finally, a kW_e-class kerosene fuel processor for SOFCs is operated.

2. Experimental

2.1. Catalysts

The reforming catalyst used in this study is a noble metal-based catalyst for high sulfur tolerances. The catalyst is Pt on Gd-doped CeO_2 (CGO–Pt) [11]. The CGO–Pt catalyst is prepared using the incipient wetness of the CGO with aqueous solutions of the corresponding metal nitrates.

There are two methods for removing the sulfur compounds in fuels. One method is a deep desulfurization over solid adsorbents (Ni-based catalyst) before the fuel reforming reaction [12]. This method has some problems, such as the catalyst reduction process, the requirement of a large-size desulfurizer due to the need for a heat supply, and difficulty of desulfurization of liquid-phase fuels. The other method for desulfurization is H_2S adsorption after the fuel reforming reaction. Removal of sulfur in the form of H_2S can be achieved by adsorption processes using absorbent materials, e.g., activated carbon and zinc oxide (ZnO) catalyst beds. The absorption on activated carbon has limited application and it is not a very cost-efficient process; however, ZnO is the most commonly used absorbent to desulfurize hydrocarbon feeds with sulfur in the form of H_2S [13]. Thus, a conventional desulfurization catalyst (ZnO) for removing the H_2S in the reformate gas is obtained from Süd-Chemie in the form of pellets [14]. For the microreactor reaction, 2 ml of the ATR catalyst and 1.2–3.5 ml of the desulfurization catalyst are charged in the reactor. For the kerosene ATR reactor and the kerosene fuel processor, 250 and 350 ml of the ATR catalyst, respectively, and 600 ml of the desulfurization catalyst are charged in each reactor.

2.2. Microreactor test

A schematic of the microreactor used in this study for kerosene ATR and H_2S adsorptive desulfurization reactions is shown in Fig. 1. The reactants for the kerosene ATR are fuel, water, and air. The synthetic fuel is used to observe the H_2S removal in the reformate gas as a fuel. The synthetic fuel is composed of normal dodecane (n-$C_{12}H_{26}$, 99%+, Sigma–Aldrich) and 1000 wt. ppm of dimethyl disulfide ($C_2H_6S_2$, 98%+, Sigma–Aldrich). The fuel and de-ionized water (>15 MΩ) are supplied by an high performance liquid chromatography (HPLC) pump (MOLEH Co. Ltd.). The water is supplied to a steam generator, and a small quantity of N_2 is fed into the steam generator to obtain a stable steam flow. The air and N_2 are metered using a mass flow controller (MKS Co. Ltd). The ATR and desulfurization reactors are made from a 12.7 mm STS (stainless steel) tube and placed inside an electrical furnace. They are controlled using a PID temperature controller and monitored by two thermocouples placed at the top and bottom of the catalyst.

The kerosene ATR reactions are carried out at O_2/C ratio = 0.7 and H_2O/C = 2, with a synthetic fuel feed. The gas hourly space velocity (GHSV) of 12,500 h^{-1} is selected based on previous studies [15–17], and the temperature of the electrical furnace is set at 800 °C. The desulfurization study is performed in a variety of reaction conditions, including various catalyst volumes and electrical

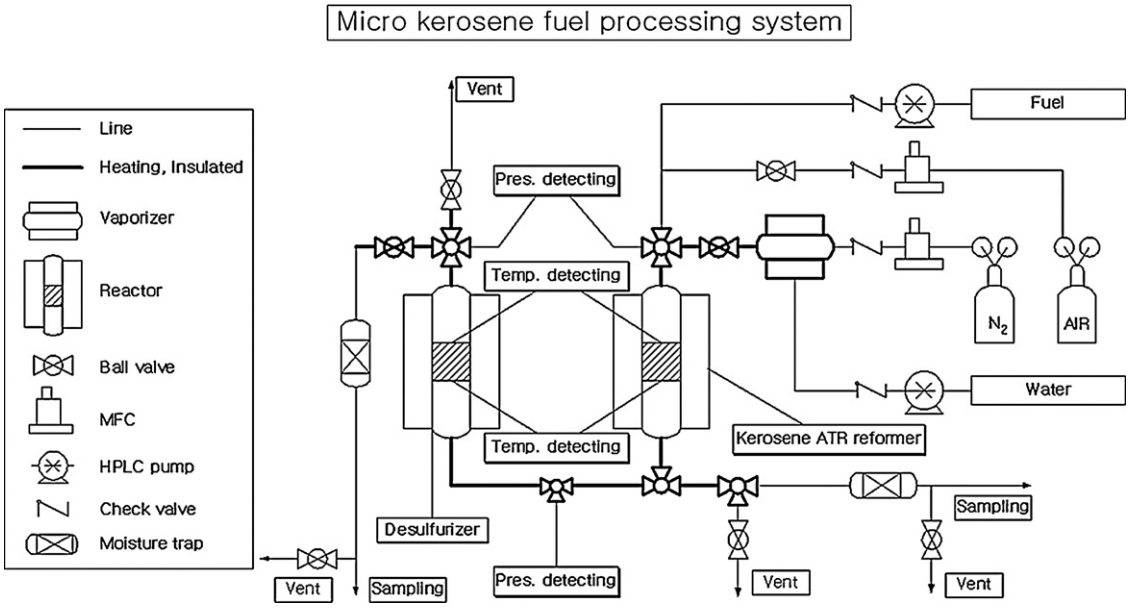

Fig. 1. Schematic diagram of the microreactor system.

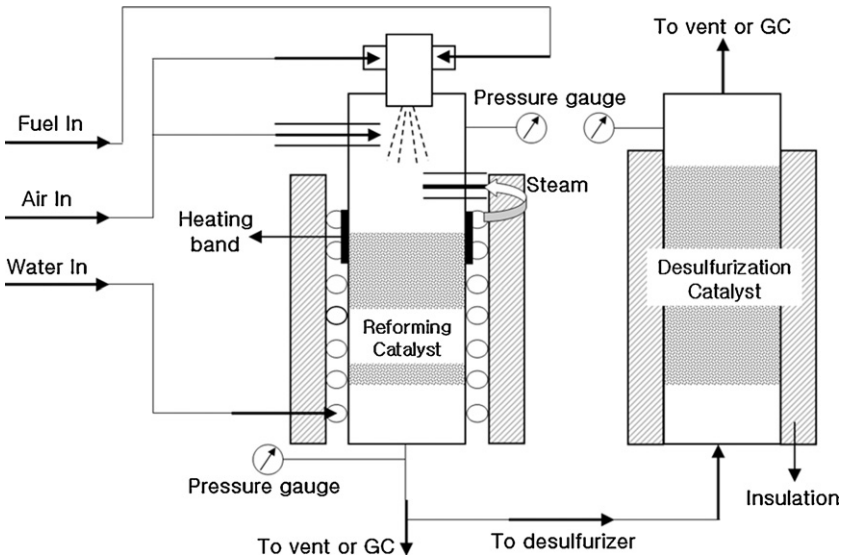

Fig. 2. Schematic of the apparatus for testing the fuel processor.

furnace temperatures. We indicate the reaction conditions of all experiments in each figure caption.

2.3. kW_e-class kerosene fuel processor operation

The temperature of the desulfurization reactor has to be maintained under 600 °C during SOFC operation to sufficiently remove the H_2S. Thus, we first investigate the self-sustaining kerosene ATR reactor to measure the temperature of the kerosene reformate gas. Fig. 2 shows a schematic of the self-sustaining kerosene fuel processor. Five sealed thermocouples are located at the center of each reactor, as shown in Fig. 3. The twin-fluid nozzle is located at the top of the reactor. A water line for vaporization is in contact with the ATR reactor wall as a coiled spring. A fraction of the air used in the ATR reaction is injected through a twin-fluid nozzle, and the residual air is supplied to the reactor. Between the reactor and the heat insulator, a heating-band is used as an igniter, which is only turned on to light the catalytic reaction during the start-up of the reactor. Commercial kerosene (SK-energy, Korea) is used as the fuel. The DC-controllable RHB pump (Fluid Metering Inc.) is used as a fuel and water pump. The kW_e self-sustaining kerosene fuel processor is then operated. The kerosene fuel processor used in this study incorporates kerosene ATR and desulfurizer.

2.4. Analytical

The water present in the product, post-reformate, and desulfurization gases is removed using a moisture trap, and the gases are then analyzed by gas chromatography (Agilent 6890N), which consists of a thermal conductivity detector (TCD), an flame ionization detector (FID), and a pulsed flame photometric detector (PFPD). The concentrations of H_2, CO, CO_2, O_2, and N_2 are determined with the TCD. The FID can analyze the relative amounts of hydrocarbons (CH_4, C_2H_2, C_2H_4, C_2H_6, C_3H_6, C_3H_8, i-C_4H_{10}, and n-C_4H_{10}). Sulfur compounds that include H_2S in the product gases are detected by the PFPD.

The synthetic fuel conversion is expressed in Eq. (3). Because of practical analytic limitations [3], the fuel conversion of the reforming experiment using synthetic diesel is calculated based on a carbon balance between the inlet and the outlet. However, the fuel conversion cannot be calculated for the commercial kerosene reforming because of the lack of information regarding the correct

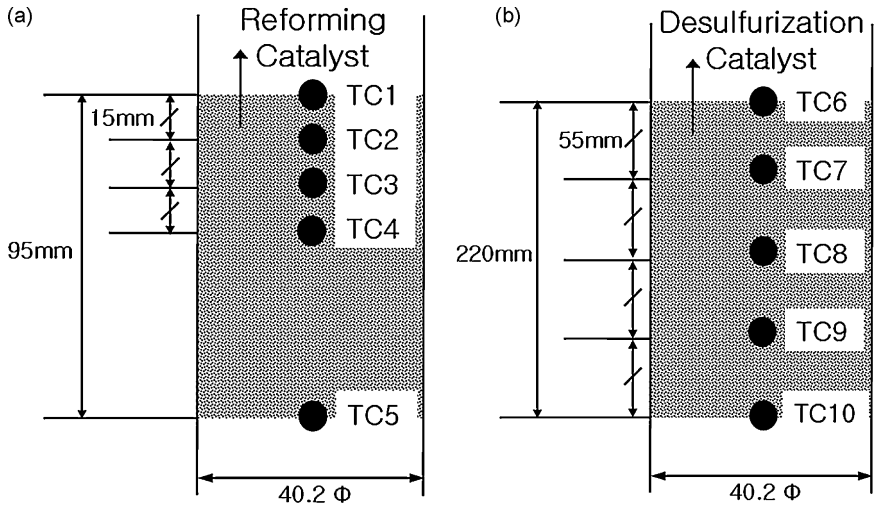

Fig. 3. Positions of the thermocouples in the (a) reformer and (b) desulfurizer.

chemical formula. The reforming efficiency and the H_2S conversion are defined in Eqs. (4) and (5) [5]:

$$\text{fuel conversion}\,(\%) = \frac{\text{total number of carbon CO, } CO_2\text{, and } CH_4 \text{ in product}}{\text{carbon number in fuel used}} \times 100 \quad (3)$$

$$\text{reforming efficiency}\,(\%) = \frac{\text{LHV of}\,(H_2 + CO)}{\text{LHV of fuel}} \times 100 \quad (4)$$

$$H_2S\ \text{conversion}\,(\%) = \frac{H_2S\ \text{mole in inlet gas} - H_2S\ \text{mole in outlet gas}}{H_2S\ \text{mole in inlet gas}} \times 100 \quad (5)$$

3. Results and discussion

3.1. Microreactor reaction

In our previous work, we carried out ATR reactions of several liquid hydrocarbon fuels and investigated the effect of the reaction conditions such as the reaction temperature, the O_2/C ratio, and the H_2O/C ratio [15–17]. It was shown that favorable reaction conditions were a temperature of the kerosene ATR reaction of about 800 °C, an O_2/C ratio of 0.7, a H_2O/C ratio of 2, and a GHSV of 12,500 h^{-1}. However, some papers reported that, although the Pt catalyst is more sulfur-tolerant compared to a Ni catalyst, it is still being poisoned at even low ppm. Thus, we study the sulfur tolerance of the CGO–Pt ATR catalyst. Two milliliters of catalyst for the ATR reaction are loaded in the reformer. Fig. 4 shows the tolerance test of the ATR reaction catalyst (CGO–Pt) for a synthetic fuel (mixed with n-$C_{12}H_{26}$ and 1000 wt. ppm of $C_2H_6S_2$) at 800 °C with molar ratios of O_2/C = 0.7 and H_2O/C ratio = 2 over 50 h. The conversion of the synthetic fuel has not decreased after about 60 h, and variations of the reformate gas distribution are not detected. The H_2S concentration is about 82 vol. ppm in the reformate gas.

The H_2S removal experiment is then performed. We investigate the effects of the GHSV and the temperature of the desulfurization reaction with the ZnO catalyst. Three-and-a-half milliliters of desulfurization catalyst are loaded into the desulfurizer to investigate the effects of the reaction temperature. The amounts of product gases from the ATR reformer and desulfurizer are shown in Fig. 5 as functions of the desulfurization reaction temperature. The amounts of H_2 and CO_2 from the desulfurization product gas increase more than those of the ATR product gas. The amounts of H_2 and CO_2 increase as the desulfurization temperature is increased from 300

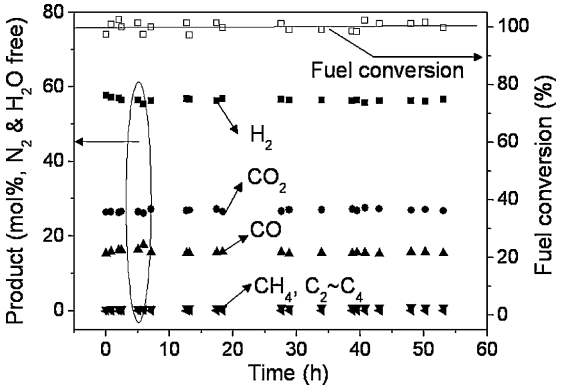

Fig. 4. Conversion and distribution of the reformate gas vs. operating time, reforming catalyst vol. = 2 ml, GHSV = 12,500 h^{-1}, H_2O/C = 2, O_2/C = 0.7, reforming reaction temperature = 800 °C.

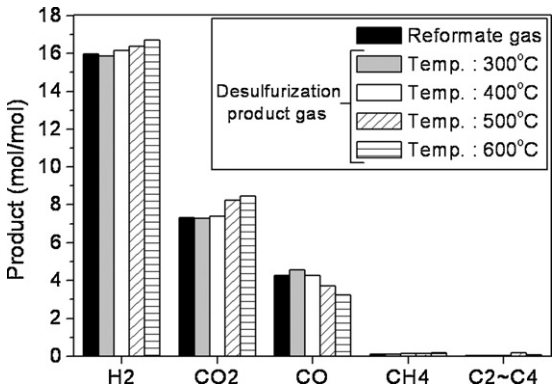

Fig. 5. Product distribution from the ATR and the desulfurization at several desulfurization reaction temperatures; reforming catalyst vol. = 2 ml, GHSV = 12,500 h^{-1}, H_2O/C = 2, O_2/C = 0.7, reforming reaction temperature = 800 °C, desulfurization catalyst vol. = 3.5 ml.

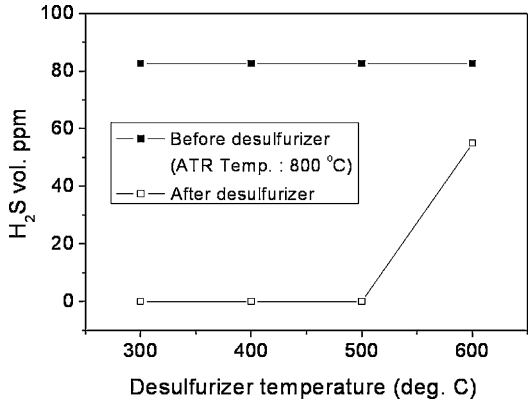

Fig. 6. H_2S concentration in the product gas of the desulfurization vs. temperature.

to 600 °C, whereas the CO amount in the product gas decreases with increasing temperature. These phenomena are caused by a WGS reaction in the desulfurizer. The product gas from the ATR reacts not only during the adsorptive desulfurization reaction of the H_2S and ZnO catalyst but also during WGS reactions of CO and H_2O due to the reaction temperature. The concentration of H_2S in the product gas from the desulfurizer as a function of the desulfurization temperature is shown in Fig. 6. H_2S is not detected as the reaction temperature is increased from 300 to 500 °C, but the amount of H_2S is found to be about 55 ppm at 600 °C. The concentration and conversion of the H_2S from the desulfurizer is carried out for reaction temperatures shown in Table 1. We know that the temperature of the desulfurization must be kept under 600 °C for sulfur removal in this experiment.

In addition, the effect of the GHSV in the desulfurizer is investigated. The reaction temperature is set to 400 °C, and the catalyst is loaded with a volume ranging from 1.2 to 3 ml. The relationship between the catalyst and the reformate gas volume is calculated according to the GHSV, and the range of the GHSV in the desulfurizer is 10,000–30,000 h^{-1}. Fig. 7 shows the concentration of H_2S in the product gas of the desulfurizer as a function of the desul-

Table 1
H_2S concentration and conversion as functions of the reaction temperature.

Reaction temperature	Concentration (vol. ppm)	Conversion (%)
300 °C	0	100
400 °C	0	100
500 °C	0	100
600 °C	55.2	33.3

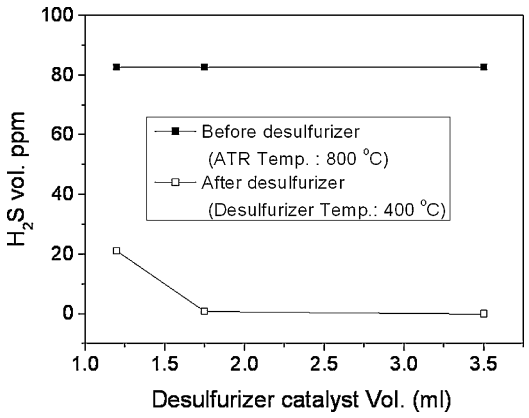

Fig. 7. H_2S concentration in the product gas of the desulfurization reaction vs. desulfurization catalyst volume; reforming catalyst vol. = 2 ml, GHSV = 12,500 h^{-1}, $H_2O/C = 2$, $O_2/C = 0.7$, reforming reaction temperature = 800 °C, desulfurization reaction temperature = 400 °C.

Table 2
H_2S concentration and conversion as functions of the catalyst volume.

Catalyst vol. (ml)	GHSV in desulfurizer (h^{-1})	Concentration (vol. ppm)	Conversion (%)
1.2	~30,000	21	74
1.75	~20,000	0.88	98
3.5	~10,000	0	100

furization catalyst volume. The H_2S is not detected after 3.5 ml of desulfurization catalyst is added, and the product gas contains a very low concentration of H_2S (about 0.88 ppm) for 1.75 ml of catalyst. However, H_2S is found at relatively high concentrations (about 21 ppm) for 1.2 ml of catalyst. This result shows that the H_2S adsorption on the catalyst is not sufficient at high space velocities (more than about 20,000 h^{-1}) and that a suitable range of GHSV is between 10,000 and 20,000 h^{-1} to obtain an efficient and stable H_2S removal in the reformate gas. The H_2S concentration and conversion in the product gas are performed using different catalyst volumes (GHSV variation), as summarized in Table 2.

3.2. Operation of kW_e self-sustaining kerosene fuel processor

Before the 2 kW_e-class kerosene fuel processor operation, an individual 1 kW_e ATR reactor is tested, where 250 ml of a CGO–Pt catalyst are loaded. Table 3 illustrates some properties of the kerosene used in this experiment. In our previous work, the start-up process of the reformer was studied [18]. Reforming reactants essentially passed through the thermodynamic coke formation region during the reforming start-up [16]. Therefore, rapid start-up protocols and conditions are required to minimize coke formation. We select the protocol of the reforming start-up using total combustion between the kerosene and the air because the total combustion methodology can suppress carbon deposition. Firstly, the start-up is initiated by a heating-band, which is installed on the external wall of the reformer. This heating-band supplies heat energy until the temperature of the inlet section of the catalyst bed reaches about

Table 3
Properties of kerosene.

Contents	Unit	Value
LHV (lower heating value)	J g^{-1}	46,110
HHV (higher heating value)	J g^{-1}	42,980
Density	kg m^{-3}	792.1
Amount of aromatics	wt.%	19.6
Amount of sulfur compounds	wt. ppm	6

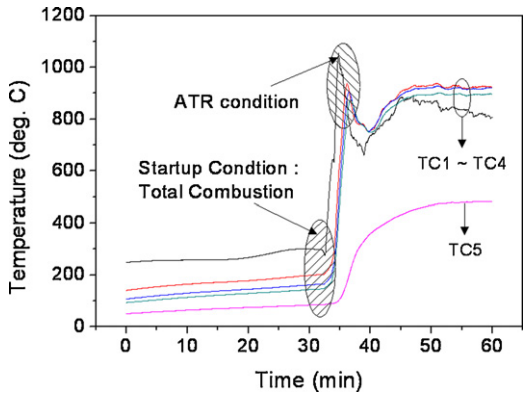

Fig. 8. Temperature profile in the reforming catalyst during the reformer start-up.

200–250 °C. The kerosene and the air are then fed for total combustion conditions [Eq. (6)]. The kerosene and the air are supplied at 0.253 ml min^{-1} and 25.7 l min^{-1}, respectively. Several minutes later (about 3–5 min), the flow rate is switched from total combustion conditions to ATR conditions. The kerosene ATR reactor runs are conducted for a GHSV of 12,500 h^{-1} and feed molar ratios of $H_2O/C = 2$ and $O_2/C = 0.68$, similar to the conditions of microreactor reactions. The start-up protocol and the catalyst bed temperature of the kerosene-reforming reactor are presented in Fig. 8:

$$C_nH_m + (n + m/4)O_2 = nCO_2 + (m/2)H_2O \quad (6)$$

Fig. 9 shows the reactor axial temperature profile during the 1 kW_e kerosene ATR. There is a temperature difference of more than 400 °C between the catalyst inlet and outlet. The exothermic reaction from the kerosene oxidation is nearly completed at the inlet section of the catalyst bed when the sequential endothermic reaction from the steam reforming occurs in the next catalyst section. During the ATR reaction, it is known that the heat energy coming from the exothermic reaction during the fuel oxidation leads to a sequential endothermic reaction of the SR [5]. Most of the kerosene is decomposed during the oxidation reaction, and SR reactions involving unreacted light hydrocarbons continue through the remaining section of the catalyst [19]. We have shown the feasibility of desulfurizer operations without a heat exchanger at a proper temperature for H_2S removal, namely, when the temperature of the reformer tail gas is about 500–550 °C and is suitable for adsorptive desulfurization on the ZnO catalyst.

The reforming efficiency and the distribution of the reformate gas after 140 h are given in Fig. 10. The reforming efficiency is about 55–60%. The product gas equilibrium concentration and reforming efficiency of the experimental ATR condition for kerosene

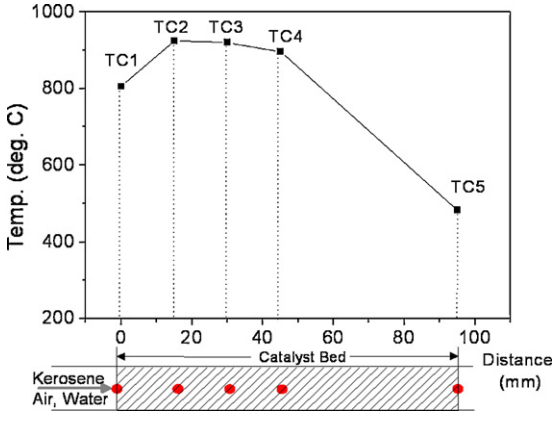

Fig. 9. Temperature profile in the reforming catalyst during steady state.

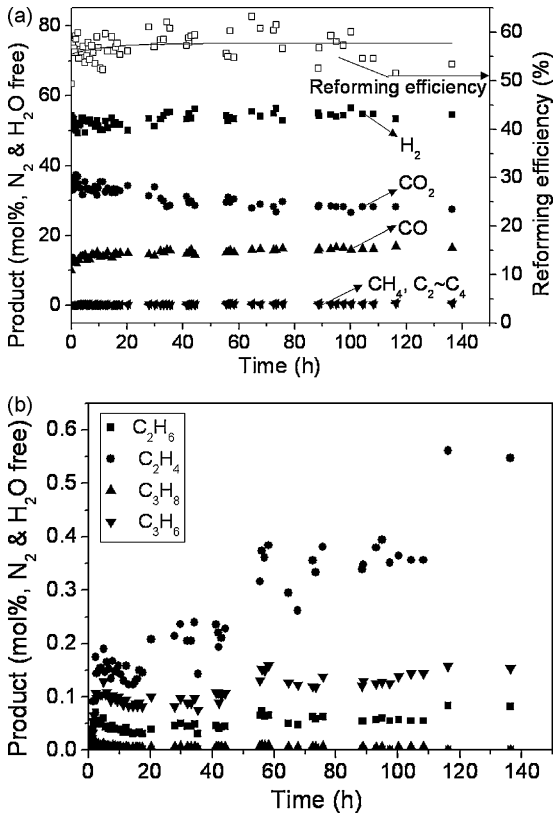

Fig. 10. (a) Reforming efficiency and production distribution and (b) light hydrocarbon distribution vs. operating time during 1 kW_e autothermal reforming of kerosene; catalyst vol. = 250 ml, GHSV = 12,500 h^{-1}, $O_2/C = 0.68$, $H_2O/C = 2$.

are shown in Fig. 11. The equilibrium compositions are obtained by using the HSC chemistry software package (ver. 5.1), which is based on the Gibbs energy minimization method. n-$C_{12}H_{26}$ is used as a surrogate of kerosene for the thermodynamic estimation. Thermodynamic estimation of product distribution and reforming efficiency is similar to the experimental results at 550 °C.

However, a slight decrease of the H_2 and CO yields is observed and no pressure drop between the catalyst inlet and outlet sections is found during the reactor operation time. The amount of unreacted light hydrocarbons, especially ethylene, a representative of carbon precursor, increased with increasing operation time. This phenomenon indicates an increase in carbon deposition in the ATR reactor due to incomplete mixing of all feed gas components, especially between steam and the other reactants.

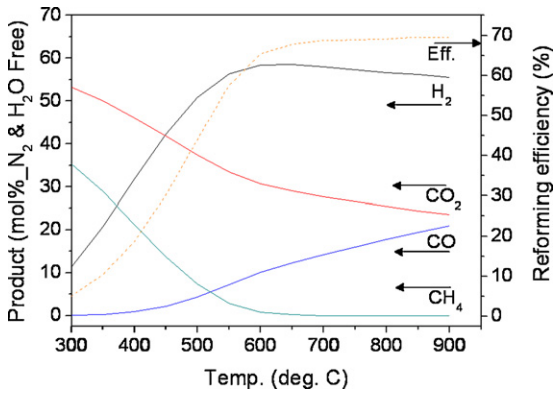

Fig. 11. Thermodynamic equilibrium of n-dodecane ATR; $O_2/C = 0.68$, $H_2O/C = 2$.

Table 4
Volumetric flows of reformate components.

Components	H_2	CO	CO_2	CH_4	H_2O	C_2–C_4
Amounts (l min^{-1})	14.1	5.7	8.5	0.7	32.3	1.0

Finally, we operate the 2 kW_e-class self-sustaining kerosene fuel processor based on individual kerosene ATR experiments, where 350 ml of reforming catalyst (CGO–Pt) and 600 ml of desulfurization catalyst (ZnO) are loaded in each reactor. The start-up protocols and reforming conditions of the kerosene fuel processor are the same as those used for previous 1 kW_e ATR reactors. Electric equipment for heat supply and fuel or water vaporization is not used in this fuel processor, with the exception of the heating-band for reformer start-up, due to the exothermicity of the ATR reformer and desulfurizer. Additionally, a heat exchanger is not required between the ATR reformer and the desulfurizer because the ATR tail gas is suitable for the adsorption of H_2S on the ZnO catalyst beds. Because of lower temperature of ATR reformate, CH_4 concentration in product gas is higher. However, unlike low-temperature fuel cells, SOFCs can directly use CH_4 as a fuel in addition to sufficient steam feeds. In our previous research, CH_4 could be internally reformed very well by an electrochemical reaction between CH_4 and steam on the anode at $H_2O/CH_4 \geq 1.5$ [20]. The absolute amounts of the reformate of kerosene fuel processor are presented in Table 4. Steam amount in the reformate is sufficient for internal reforming of CH_4 on the anode of SOFCs.

The reformer is run at a hydrogen and carbon monoxide throughput of about 20 l min^{-1} for 250 h using commercial kerosene as fuel. The reforming efficiency and distribution of the product gas during fuel processor operation times are given in

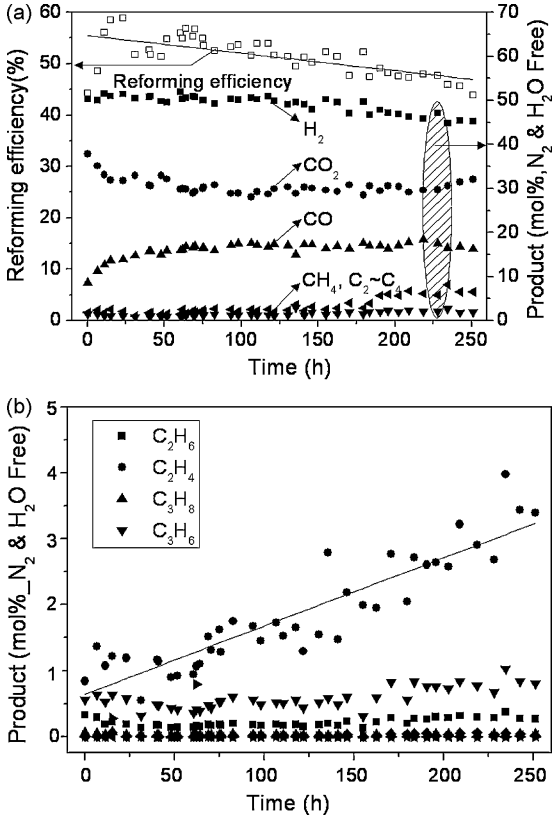

Fig. 12. (a) Reforming efficiency and production distribution and (b) light hydrocarbon distribution vs. operating time during operation of the kerosene 2 kW_e fuel processor; reforming catalyst vol. = 350 ml, GHSV = 12,500 h^{-1}, $O_2/C = 0.68$, $H_2O/C = 2$, desulfurizer catalyst vol. = 600 ml.

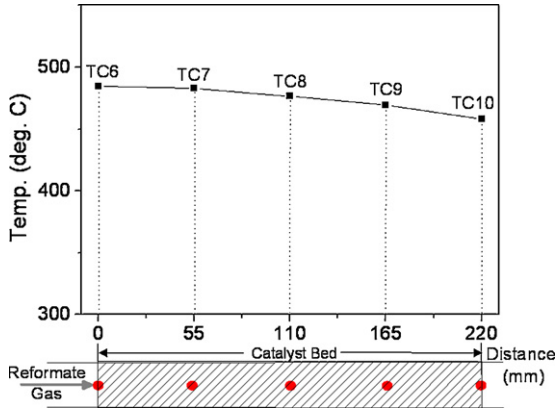

Fig. 13. Temperature profile in the desulfurization catalyst.

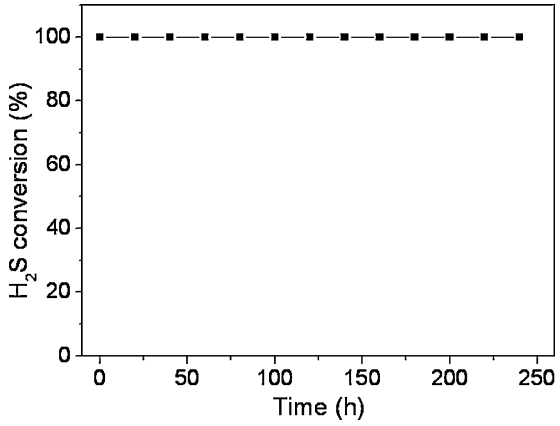

Fig. 14. H_2S conversion vs. operating time.

Fig. 12. In contrast to the 1 kW_e ATR reactor test, the performance of the fuel processor gradually decreases from around 65% to 55%. The degradation of reforming performance is caused by carbon deposition due to incomplete mixing of reactants. As can be seen in Fig. 12(b), the concentration of ethylene, a representative carbon precursor, increases with increasing operation times. The gradual increase of carbon deposition on the reforming catalyst leads to a continuous decrease in the activity of the catalyst. In addition, the carbon deposition on the SOFC anode is induced by the ethylene present in the product gas of the fuel processor. A carbon-tolerant catalyst for liquid fuel (high hydrocarbon fuels) reforming, mixing enhancement of all feed gas reactants, and the removal of the light hydrocarbons in the products will be studied in future work for stable operations of the fuel processor and the SOFCs. However, the desulfurizer is successfully run for 250 h. Fig. 13 shows the desulfurizer axial temperature profile. There is no significant temperature difference between the catalyst inlet and outlet sections, and self-sustaining operation of the desulfurizer is made possible due to the slightly exothermic desulfurization reaction. The H_2S present in the product gas is not detected during fuel processor operations. The H_2S conversion is shown in Fig. 14. These results show the stable operation of the desulfurizer.

4. Conclusion

Micro-reformers and desulfurizers are investigated for operation of integrated fuel processors that are charged with a sulfur-tolerant catalyst (CGO–Pt) for ATR and ZnO desulfurizations. The reforming performance is not affected, and ZnO allows full removal of the hydrogen sulfide at temperatures ranging from 300 to 500 °C and for a GHSV range between 10,000 and 20,000 h^{-1}. The self-sustaining integrated fuel processor is run continuously for 250 h at a 2 kW_e-class output gas (hydrogen and carbon monoxide throughput of about 20 l min^{-1}) for SOFC operations using a kerosene fuel. This fuel processor does not require electric equipment and heat exchanger for heat supply or vaporization of fuel or water. The observed decreasing temperature profile of the ATR catalyst bed is in agreement with the mechanisms of sequential reaction. Indeed, the energy from the exothermic reaction of the fuel oxidation leads to sequential endothermic reactions of the SR reaction. Thus, the temperature of ATR tail gas is suitable for the adsorptive desulfurization reaction. CH_4 concentration in product gas is higher due to lower temperature of ATR reformate. The kerosene fuel processor is designed for operation of SOFCs in this study, so it is possible to use the CH_4 from the reformate in SOFCs due to the electrochemical reaction between CH_4 and steam at the anode of SOFCs. Though the fuel processor performance gradually decreases, the reforming efficiency is about 60%, and the desulfurizer allowed removal of sufficient levels of H_2S to operate SOFCs.

Acknowledgments

This work was funded by the Korea Electric Power Research Institute (KEPRI) and the Korean Government. Analysis facilities, such as the GC–MS and SEM/EDX, were supported by the Ministry of Education and Human Resources Development. In addition, this work is an outcome of the projects of the Best Lab. Program by the Ministry of Commence, Industry, and Energy (MOCIE).

References

[1] L. Barreto, A. Makihira, K. Riahi, Int. J. Hydrogen Energy 28 (2003) 267–284.
[2] M. Momirlan, T.N. Veziroglu, Int. J. Hydrgen Energy 30 (2005) 795–802.
[3] A. Qi, S. Wang, C. Ni, D. Wu, Int. J. Hydrogen Energy 32 (2007) 981–991.
[4] M. Ferrandon, J. Mawdsley, T. Krause, Appl. Catal. A: Gen. 342 (2008) 69–77.
[5] S. Ahmed, M. Krumpelt, Int. J. Hydrogen Energy 26 (2001) 291–301.
[6] J. Larminie, A. Dicks, Fuel Cell Systems Explained, second ed., Wiley, New York, 2003, pp. 1435–1439.
[7] M. Boder, R. Dittmeyer, J. Power Sources 155 (2006) 13–22.
[8] T. Takeguchia, Y. Kania, T. Yanoa, R. Kikuchia, K. Eguchia, K. Tsujimotob, Y. Uchidac, A. Uenoc, K. Omoshikic, M. Aizawa, J. Power Sources 112 (2002) 588–595.
[9] A. Docter, A. Lamm, J. Power Sources 84 (1999) 194–200.
[10] C.H. Bartholomew, P.K. Agrawal, J.R. Katzer, Adv. Catal. 31 (1982) 135–242.
[11] M. Krumpelt, T.-R. Krause, J.-D. Carter, J.-P. Kopasz, S. Ahmed, Catal. Today 77 (2002) 3–16.
[12] X. Ma, S. Velu, J.-H. Kim, C. Song, Appl. Catal. B: Environ. 56 (2005) 137–147.
[13] A. Hidalgo-Vivas, B.H. Cooper, In Handbook of Fuel Cells, vol. 3, John Wiley & Sons Ltd., Chichester, 2003, pp. 177–189.
[14] Y.-S. Yoon, M.-J. Kim, Energy Fuels 21 (2007) 3537–3540.
[15] I.-Y. Kang, J.-M. Bae, G.-J. Bae, J. Power Sources 163 (2006) 538–546.
[16] I.-Y. Kang, J.-M. Bae, J. Power Sources 159 (2006) 1283–1290.
[17] S.-H. Yoon, I.-Y. Kang, J.-M. Bae, Int. J. Hydrogen Energy 34 (2009) 1844–1851.
[18] I.-Y. Kang, J.-M. Bae, S.-H. Yoon, Y.-S. Yoo, J. Power Sources 1772 (2007) 845–852.
[19] D.-J. Liu, T.-D. Kaun, H.-K. Liao, S. Ahmed, Int. J. Hydrogen Energy 29 (2004) 1035–1046.
[20] I.-Y. Kang, Y.-H. Kang, S.-H. Yoon, G.-J. Bae, J.-M. Bae, Int. J. Hydrogen Energy 33 (2008) 6298–6307.